Output Filter Aware Optimization of the Noise Shaping Properties of ΔΣ Modulators via Semi-Definite Programming

Sergio Callegari, *Senior Member, IEEE* and Federico Bizzarri, *Member, IEEE*

arXiv:1302.3020v2 [cs.IT] 24 Sep 2013

***Abstract*—The Noise Transfer Function (NTF) of ΔΣ modulators is typically designed after the features of the input signal. We suggest that in many applications, and notably those involving D/D and D/A conversion or actuation, the NTF should instead be shaped after the properties of the output/reconstruction filter. To this aim, we propose a framework for optimal design based on the Kalman–Yakubovich–Popov (KYP) lemma and semi-definite programming. Some examples illustrate how in practical cases the proposed strategy can outperform more standard approaches.**

***Index Terms*—Delta-Sigma Modulation, Semi-definite Programming, Optimization.**

I. Introduction

ΔΣ modulators [1]–[4] are nowadays widely used in a variety of systems, usually as analog to digital (A/D) and digital to digital (D/D) interfaces. The latter may in turn simplify sample rate conversion, digital to analog (D/A) conversion, or power amplification in actuation tasks. Typical applications range from data conversion itself to signal processing in wide sense, including digital audio [5], frequency synthesis [6], switched mode amplification [7], [8], power conversion and actuation [9], [10], digital communications [8], [11], sensing [12] and more. Recently, more exotic applications, such as in optimization, have been proposed too [13]–[15].

ΔΣ modulators are signal encoders (or re-coders) capable of trading rate for accuracy in order to translate high-resolution slowly (or non) sampled signals into low-resolution rapidly sampled signals with little loss of fidelity. This property is achieved through a feedback architecture involving a quantizer and linear filters which provide *noise shaping*, i.e., the ability to unevenly distribute the quantization noise power so that some frequency bands get most of it and others almost none.

ΔΣ modulators are almost invariably used in conjunction with filters as in Fig. 1, to recover useful information that is otherwise polluted by quantization noise. In fact, the digital stream at the output of the modulator has a much wider bandwidth than the input waveform, thanks to its high sampling rate (oversampling). Furthermore, it contains two components. The first one reflects the input signal itself, thus occupying just the set of frequencies $\mathcal{B}$ constituting the signal band. The second one is quantization noise, whose power is approximately fixed, depending on the quantizer resolution. In principle, the noise Power Density Spectrum (PDS) extends throughout all the available bandwidth. Actually, the modulator lets the noise PDS concentrate more in certain regions than in others. If these regions do not overlap with $\mathcal{B}$, then a filter can be used to get rid of (most of the) noise component without affecting the signal one. These considerations make evident how an output or reconstruction filter is mandatory. Indeed, the modulator role is precisely to *shape the noise* so that it can be made *orthogonal* to the signal (and thus linearly separable). Fig. 2 shows the typical behavior in the frequency domain for a modulator suitable for Low-Pass (LP) signals (f_Φ indicates the modulator output rate). Fig. 3 shows some specializations of the generic architecture to binary A/D conversion, D/A conversion and switched-mode power amplification.

The above premises explain why typical design flows [3], [16], [17] want the modulator noise shaping properties to be based only on the signal features (and notably the width of $\mathcal{B}$). To be separable from the signal, the quantization noise needs just to be as *orthogonal* as possible to it. Hence, typical flows let the modulator shape its noise PDS so that it is as low as possible in the signal band and (consequently) high elsewhere,

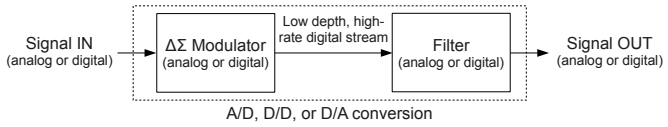

Figure 1. Typical deployment of a ΔΣ modulator.

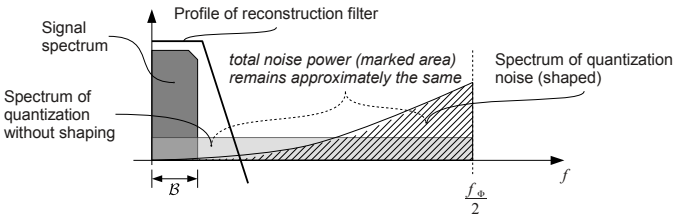

Figure 2. Typical noise shaping and noise removal in a LP ΔΣ modulator.

This is a post-print version of a paper published in the IEEE Transactions on Circuits and Systems — Part I, Vol. 60, N. 9, pp. 2352 - 2365, Sept. 2013. Available through DOI 10.1109/TCSI.2013.2239091. Always cite as the published version.

Copyright © 2013 IEEE. Personal use of this material is permitted. However, permission to use this material for any other purposes must be obtained from the IEEE by sending a request to pubs-permissions@ieee.org.

S. Callegari is with the Department of Electrical, Electronic, and Information Engineering "Guglielmo Marconi" (DEI) and the Advanced Research Center on Electronic Systems for Information and Communication Technologies "E. De Castro" (ARCES) at the University of Bologna, Cesena 47521, Italy. E-mail: sergio.callegari@unibo.it.

F. Bizzarri is with the Dipartimento di Elettronica, Informazione e Bioingegneria, Politecnico di Milano, Italy. E-mail: bizzarri@elet.polimi.it.

with a transition between the two regions as steep as possible to prevent superposition. Indeed, this is what *theoretically* enables the most thorough noise separation.

However, the fact that two items are *theoretically* well separable does not mean that they necessarily get well separated *in practice*. Typical design flows assure that a linear filter exists capable of guaranteeing an almost perfect noise removal. Nevertheless, they cannot assure that such filter is actually deployed. As a matter of fact, there are favourable situations where the designer has very good control over the output filter. In this case, conventional design flows are probably optimal. For instance, in A/D conversion (Fig. 3a) the output filter is digital so that a good filter can be implemented without excessive cost. In other cases, the designer has only a limited control over the output filter. For instance, in D/A conversion (Fig. 3b), one has an analog reconstruction filter whose cost may rapidly grow with its specification (in particular with roll-off). This situation may also arise in signal synthesis [18]. Even worse, there may be cases where the filter is in part pre-assigned leaving the designer with extremely limited or no control at all over it. For instance, in actuation (Fig. 3c) the filter is often partially (if not completely) provided by the electric machine used for the actuation itself. As an example, consider that the popular Texas Instruments LM4670 switching audio amplifier is marketed as a *filterless* solution where the LP filter is provided by the speaker parasitic inductance and inertia (and possibly by the listener's ear) [19]. A similar situation may arise in ac motor drives [20], [21].

We claim that whenever the designer has limited or no control over the output filter, the noise shaping properties of the ΔΣ modulator should not be designed after the signal properties alone. Conversely, the designer, aware of the limitations induced by a sub-optimal output filter, should explicitly consider them to pursue the best possible reduction of the quantization noise. In the following Sections, we formalize this claim providing a novel design flow for ΔΣ modulators, based on the output filter features. Figure 4 graphically summarizes the differences between a traditional flow and ours. In the former (a), the modulator noise shaping features are designed after the signal properties alone. When these features are obtained, an *optimum* output filter is designed to take the best possible advantage of them. In other words, the output filter is not a constraint, but a degree of freedom to be exploited to make the most of the modulator noise shaping profile. In our flow (b), the first thing being assigned is the output filter, for which not just the signal properties but also other factors related to the context where the modulator is applied must be considered (as it happens in the examples in Figs. 3b and 3c). Then, the modulator noise shaping features are designed to cope at best with the filter. Thus, for us the output filter is a constraint to be managed.

The proposed approach stems from interpreting the modulator as a heuristic solver for a Filtered Approximation (FA) problem [13]. It results in a Finite Impulse Response (FIR) Noise Transfer Function (NTF), obtained via Semi-definite Programming (SDP) [22]. The restriction to FIR NTFs often results in higher order modulators than in conventional flows, but in many applications this is not an issue, as discussed in [17]. The minimization used to define the filter coefficients respects

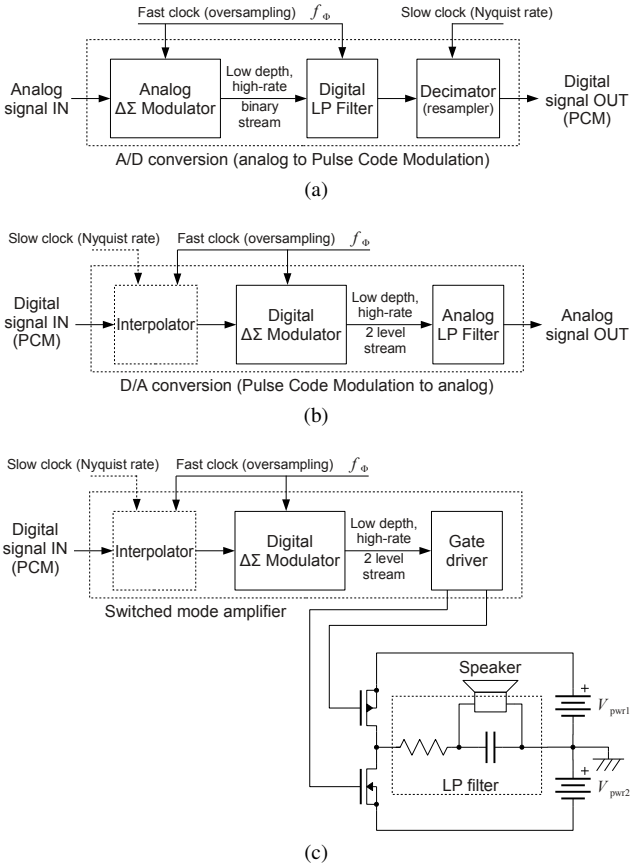

Figure 3. Specializations of the architecture in Fig. 1 for LP signals and a binary-output ΔΣ modulator: A/D converter with PCM output (a); D/A converter with PCM input (b); switched-mode amplifier with PCM input (c).

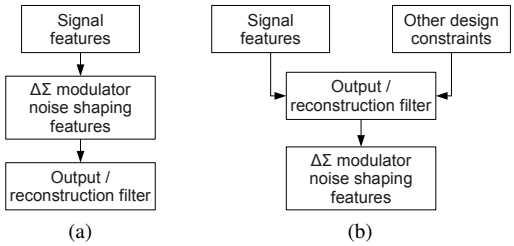

Figure 4. Traditional (a) and proposed (b) design flows.

the most important design constraints for ΔΣ modulators [3], [23], [24] and thus enables a robust design. It is formalized taking advantage of the Kalman–Yakubovich–Popov (KYP) lemma [25], [26]. This is not the first time that the KYP lemma is applied to the optimization of ΔΣ modulators, yet in precedent cases the goals of the optimization were quite different [17], [27]. Furthermore, previous attempts at considering the output filter features in the design of ΔΣ modulators are scarce and followed different strategies [28].

In the last part of the paper, we provide extensive design examples, showing how the proposed design strategy can consistently outperform conventional ones and is also much more flexible, being capable of managing all kinds of modulators, including multi-band ones, in a completely homogeneous way. Furthermore, the strategy is often more

robust. The examples show that, in conjunction with output filters lacking too steep features, it results in NTFs lacking steep features too. Consequently, as a positive side effect, one often gets less extreme modulators that tend to be less prone to misbehavior and deviation from expected performance.

II. Notation

For the sake of clarity and compactness, we make use of specific notations relative to matrices and dynamical systems.

Matrices and vectors are generally indicated by capital italic letters in a bold font as in $\boldsymbol{A}$, although for homogeneity with previous publications and the Literature some vectors may be uncapitalized as in $\boldsymbol{x}$. When it is necessary to extract a sub-matrix from a matrix, the following notation applies: $\boldsymbol{A}_{1:3,4:5}$ is the sub-matrix obtained from entries that belong to the rows from 1 to 3 and the columns from 4 to 5 in $\boldsymbol{A}$. The colon is saved if the two values on its sides are the same. For instance, $\boldsymbol{A}_{1,4:5}$ is the sub-matrix (row-vector) obtained from values in the first row and in columns from 4 to 5 in $\boldsymbol{A}$. A thick dot $\bullet$ can used as a shorthand for *beginning* or *end* depending on the side of the colon where it appears. For instance $\boldsymbol{a}_{2:\bullet}$ is a sub-vector containing entries from the second to the last one in $\boldsymbol{a}$. Coherently with the notation concepts illustrated above, $\bullet:\bullet$ can be replaced by a single thick dot to be interpreted as a shorthand for *all*. For instance, $\boldsymbol{A}_{1,\bullet}$ is the first row of $\boldsymbol{A}$. The same notation can be used to indicate matrix and vector elements. For instance, $\boldsymbol{A}_{2,1}$ is the element at the second row, first column in matrix $\boldsymbol{A}$. Note that when this kind of indexing is applied, indexes always start at 1. In cases where matrices or vectors need to be filled with values taken from other sequences, parenthesis are used as in the following example: $\boldsymbol{A} = (a_{i,j})$ for $i \in (0,\dots,7)$ and $j \in (-1,\dots,3)$ means that $\boldsymbol{A}$ is an 8×5 matrix, where $\boldsymbol{A}_{1,1} = a_{0,-1}$, and so on. When it is not otherwise declared, vectors are *column* vectors. The transposition operator $^{\mathrm{T}}$ is often used to more compactly enumerate their entries in a row, as in $\boldsymbol{a} = (a_1, a_2, a_3)^{\mathrm{T}}$.

With respect to dynamical systems, a compact matrix notation is often used for their state space model. For instance, if one has a discrete-time system $\mathcal{G}$ with model

$$\begin{cases} \boldsymbol{x}(k+1) = \boldsymbol{A}\boldsymbol{x}(k) + \boldsymbol{B}\boldsymbol{u}(k) \\ \boldsymbol{y}(k) = \boldsymbol{C}\boldsymbol{x}(k) + \boldsymbol{D}\boldsymbol{u}(k) \end{cases}$$

one may write

$$\mathcal{G} = \left(\begin{array}{c|c} \boldsymbol{A} & \boldsymbol{B} \\ \hline \boldsymbol{C} & \boldsymbol{D} \end{array}\right)(z)$$

where (z) recalls the nature of the equations, based on time differences.

III. Background

A. The ΔΣ modulator architecture and design constraints

Fig. 5a represents a generic architecture for a ΔΣ modulator including a *feedforward* filter $FF(z)$, a *feedback* filter $FB(z)$ and a quantizer. All signals are assumed discrete-time and the operation is timed by a fast clock with frequency f_Φ.

Owing to the quantizer, the modulator is hard to tackle formally. A common approach is to approximate it by the

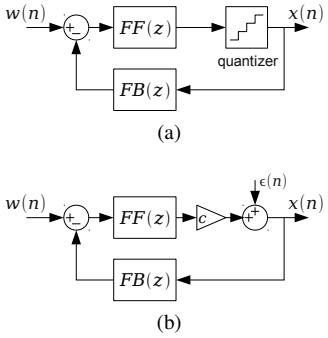

Figure 5. General ΔΣ architecture and approximate linear model.

"linearized" architecture in (b), where the quantisation noise $\epsilon(n)$ is assumed to be white and independent of the input signal. The quantity c models the *average* quantizer gain. When the loop operates correctly (namely, when the quantizer is not *overloaded*), c can be assumed approximately unitary [3], [17] as we actually take it in our discussion. In the same conditions, the quantization noise amplitude can be assumed to be half the quantization step Δ. Typically, the quantization noise distributes approximately uniformly in value, leading to a Probability Density Function (PDF) $\rho_\epsilon(x)$ approximately equal to $1/\Delta$ as long as $-\Delta/2 \leq x \leq \Delta/2$ and approximately null otherwise. This consideration enables a first, rough estimation of the input noise power in the linearized modulator, setting it at $\sigma_\epsilon^2 = \int_{-\infty}^{\infty} x^2 \rho_\epsilon(x)\ dx = \Delta^2/12$. This is the average quantization noise energy per sample. With it, the whiteness assumption on the quantization noise lets one easily express the quantization noise PDS over the normalized angular frequency axis ω as $E(\omega) = \Delta^2/12\pi$. Note that we use single sided spectra and $\omega \in [0, \pi]$.

The linearity of the approximate model is further exploited to decompose the output in the contributions due to the input and to the quantisation noise yielding $X(z) = STF(z)\,W(z) + NTF(z)\,E(z)$ where $STF(z) = FF(z)/(1+FF(z)\,FB(z))$ and $NTF(z) = 1/(1+FF(z)\,FB(z))$. Alternatively, if $STF(z)$ and $NTF(z)$ are assigned, one has

$$\begin{cases} FF(z) = \frac{STF(z)}{NTF(z)} \\ FB(z) = \frac{1-NTF(z)}{STF(z)}. \end{cases} \tag{1}$$

In typical applications, one wants the signal component to be passed from input to output without alteration, so the Signal Transfer Function (STF) is unitary, and linear phase (e.g, $STF(z) = z^{-d}$, where d is an integer delay).

It is now possible to discuss some constraints posed by the need to practically implement the loop.

1) For the stability of the linearized model, one needs the NTF to be stable (the stability of the STF is automatically guaranteed by taking it to be z^{-d}).

2) The NTF needs to be causal (the causality of the STF is automatically guaranteed by taking it to be z^{-d}).

3) $FF(z)$ and $FB(z)$ need to be causal.

4) The loop can not be algebraic. This means that $FF(z)FB(z) = (1-NTF(z))/NTF(z)$, which represents the loop transfer function, needs to be strictly causal.

Furthermore, it is necessary to observe that the conditions at point 1 are necessary and sufficient for the stability of the linearized loop, but not sufficient for the stability of the real loop, because the quantizer is strongly non-linear. Determining strict conditions for the stability of the non-linear loop is still an impossible task in general terms. However, the analysis in [3] and [17, Sec. IV-A] clearly indicate that such stability cannot be given just by the properties of the loop filters, but must necessarily depend also on the maximum amplitude that the input signal $w(n)$ takes over time, namely $\|w\|_\infty = \max_{n\in\mathbb{N}} w(n)$, so that the stability is often more difficult to achieve at large inputs. The same analysis ties the stability to the peak of the amplitude response of the NTF, indicating that the higher the peak value, the more critical the stability. Following this consideration, practical designs tend to rely on an empirical rule based on the limitation of the NTF gain (Lee criterion) [3], [24]. Hence, one has a further constraint in addition to those above:

5) The peak of the NTF amplitude response must be bounded to a low value, namely

$$\max_{\omega\in[0,\pi]} \left|NTF\left(\mathrm{e}^{j\omega}\right)\right| < \gamma \tag{2}$$

where the constant γ depends on the number of quantization levels. For binary quantizers, γ should be less than 2 and is typically set at 1.5. Incidentally, note that when a modulator turns out to overload its quantizer, it is often possible to retry its design with a lower γ. For modulators where the NTF is high-order, which are more subject to misbehavior, it is frequent to reduce γ to 1.4 or even slightly lower values. However, having to reduce γ too much also reduces the effectiveness of the NTF.

From the discussion about point 5, it should be clear that differently from the previous four, this is neither a necessary nor sufficient condition. Rather, it is just a requirement capable of making the ΔΣ modulator more *likely* to operate correctly in a wide range of practical cases.

Before proceeding to introduce design flows, it is worth mentioning that it can be convenient to slightly reword the criteria 1-4. With reference to point 4, say that the NTF is $B_{NTF}(z)/A_{NTF}(z)$. The loop function is thus $(A_{NTF}(z)-B_{NTF}(z))/A_{NTF}(z)$. To have it strictly causal, the order of $A_{NTF}(z)$ must be the same as the order of $B_{NTF}(z)$. Hence, one has

2a) The NTF needs to be causal but not strictly causal.

Furthermore, there must be cancellations (at least one) in $A_{NTF}(z) - B_{NTF}(z)$. The first cancellation can only happen if

4a) The first coefficient in the impulse response of the NTF is unitary.

If 2a is satisfied, the causality of $FF(z)$ is always guaranteed, while the causality of $FB(z)$ can certainly be guaranteed by taking $STF(z) = 1$. Hence, one can, with no loss of generality, always take $STF(z) = 1$ and consider conditions 1, 2a, 4a, 5 instead of 1-5. This makes the modulator design completely determined after the design of the NTF.

B. Conventional design flows

From the Introduction, it should be clear that common design flows place great attention to the noise present at the output of the modulator in the signal band $\mathcal{B}$. Note that $\mathcal{B}$ is a subset of the normalized angular frequency interval $[0, \pi]$ that may contain multiple sub-bands. The in-band noise power at the output of the modulator is

$$\sigma_{\mathcal{B}}^2 = \int_{\mathcal{B}} E(\omega) \left|NTF\left(\mathrm{e}^{\mathrm{i}\omega}\right)\right|^2 d\omega = \frac{\Delta^2}{12\pi} \int_{\mathcal{B}} \left|NTF\left(\mathrm{e}^{\mathrm{i}\omega}\right)\right|^2 d\omega. \tag{3}$$

For instance, in the renown case of a first order, binary LP modulator with $FF(z) = 1/z-1$ (feedforward path is an accumulator) and $FB(z) = 1$, one has $STF(z) = z^{-1}$ and $NTF(z) = 1 - z^{-1}$. The NTF is a first order differentiator having the High-Pass (HP) response

$$\left|NTF\left(\mathrm{e}^{\mathrm{i}\omega}\right)\right| = \left|1 - \mathrm{e}^{-\mathrm{i}\omega}\right| = 2\sin(\omega/2). \tag{4}$$

Letting B be the overall width of set $\mathcal{B}$ and defining the Oversampling Ratio (OSR) as $OSR = f_\Phi/2B$, in this LP case the integral in Eqn. (3) turns out to be computed on $[0, \pi/OSR]$ and thus reduces to the well known result

$$\sigma_{\mathcal{B}}^2 = \frac{\Delta^2}{12\pi} \int_0^{\pi/OSR} 4\sin^2(\omega/2)\, d\omega \approx \frac{\Delta^2}{12} \frac{\pi^2}{3OSR^3} \tag{5}$$

where the approximation is valid when the OSR is large enough. The result above can be generalized to higher order NTFs taking

$$NTF(z) = (1 - z^{-1})^P = \frac{(z-1)^P}{z^P} \tag{6}$$

i.e., making the NTF a P order differentiator (all poles in 0 and all zeros in 1). This changes Eqn. (5) into the more general

$$\sigma_{\mathcal{B}}^2 \approx \frac{\Delta^2}{12} \frac{\pi^{2P}}{(2P+1)OSR^{2P+1}}. \tag{7}$$

Three things are worth noticing: (i) the NTF in Eqn. (6) is only suitable for LP modulators; (ii) it does not respect criterion 5 (for instance the amplitude response in Eqn. (4) peaks at 4); and (iii) it does not minimize $\sigma_{\mathcal{B}}^2$.

Conventional design flows consequently aim at choosing a P order NTF minimizing the expression in (3) while respecting requirements 1, 2a, 4a, 5. Such a minimization is by no means easy and is generally practiced with approximation and iterative methods. The Literature proposes different variants. Notable ones are thoroughly described in [3] and effectively implemented in [16]. An alternative strategy still based on the signal features alone aims at a *min-max* optimization of the quantization noise, i.e., at minimizing the peak of the integrand in (3), rather than the integral itself [17].

Often, a key idea is to initially focus on a LP modulator (namely, a HP NTF), which can later be mutated into a Band-Pass (BP) modulator if needed (namely, transforming the NTF into a Band-Stop (BS) transfer function). Intuitively, a starting point can be Eqn. (6), which satisfies requirement 4a. The zeros can then be moved away from $z = 1$ (dc) to spread them onto the portion of the unit circle corresponding to frequency values from 0 to π/OSR. This guarantees that the NTF can remain more uniformly low in the signal band. An optimal zero placement can be obtained by considering (3) for an NTF

with P zeros placed onto the unit circle and by nulling its gradient taken with respect to such zeros. In [3] optimal values are tabled for $P = 1, \ldots, 8$. A second step is to push the poles away from 0 closer to $z = 1$, letting them lay within the unit circle onto a curve surrounding $z = 1$ and confining the portion of the unit circle corresponding to the signal bandwidth. This has the effect of limiting the gain of the NTF out of the signal band and is instrumental in respecting requirement 5. Some common assumptions used in this optimization are that: (i) the zeros of the NTF can be assigned (almost) independently of the poles (namely, the poles have negligible effect on the in-band noise or, alternatively, the denominator of the NTF has an almost flat response in the signal band); and (ii) requirement 5 can be verified by assuming that the NTF peaks at $\omega = \pi$.

As an example, the approach above is implemented in the `synthesizeNTF` function in the well known DELSIG toolbox [16]. The idea is to take the NTF zeros in $z = 1$ or to spread them according to the minimization procedure described above and then to take the poles of the NTF so that they correspond to a maximally flat LP filter. The bandwidth of the filter implied by the poles is then adjusted until requirement 5 is satisfied. In practice an independent optimization of the zeros and the poles of the NTF is practiced, which may lead to some issues for particular design specifications [3, Sec. 8.1].

A slight generalization of this procedure consists in choosing an NTF approximation type (e.g., Butterworth, inverse Chebyshev, etc.), and designing a HP NTF so that it is in the form $\prod_{i=1}^{P} {(z-z_i)}/{(z-p_i)}$, where z_i and p_i are the zeros and poles (so as to satisfy requirements 2a and 4a), and it has a cut-off angular frequency ω_t [1, Sec. 4.4.1]. Initially ω_t is set just slightly above the upper edge of the signal bandwidth. Then, the value of $|NTF(-1)|$ is verified and the filter is iteratively re-designed with different values of ω_t, until condition 5 is fulfilled. This means reducing ω_t if the NTF peaks at too high values and enlarging it otherwise. For some filter forms, alternatively to (or together with) ω_t, the stop-band gain (or ripple) can be used as a degree of freedom to satisfy condition 5. For instance, the DELSIG `synthesizeChebyshevNTF` uses an inverse Chebyshev form (i.e., Chebyshev filter with ripple in the stopband) [16].

As a final remark, note that the most recent design flows may rely on more sophisticated optimization strategies [17], but still base them on the signal features (namely, on $\mathcal{B}$) alone.

C. Criticism of conventional design flows

Here we briefly summarize some potential issues with conventional design flows.

a) Conventional flows share a major trait in assuming that a modulator would be *perfect* if it could push all the quantization noise away from the signal band. However, ΔΣ modulators are almost always used together with output/reconstructions filters as in Figs. 1 and 3. Thus, this view of perfection in the modulator implies another assumption of perfection on the filter side. For a perfect modulator, the modulator+filter ensemble can work optimally only if the filter can let through all that is in the signal band and reject all that is outside. Unfortunately, this on-off behavior is impossible to implement. When the output filter is imperfect, a modulator that is perfect under this standard can lead to an overall modulator+filter behavior worse than that of an imperfect modulator. Thus, in many cases one is better off adopting a different view of perfection, taking into account the features of the output filter from the very start. This is particularly important in cases like those in Figs. 3b and 3c where the output filter is analog and its specifications cannot be made too strict without incurring into high costs. Nonetheless, even in cases like Fig. 3a, where the output filter is digital, taking its response into account can be beneficial. In fact, the filter is functional to decimation and the out-of-band noise that may leak out of it is no less important than the in-band noise since the decimator/resampler aliases it onto the signal band.

b) Many conventional design flows, where the location of the NTF zeros is decided independently from the NTF poles, provide good results only if the denominator polynomial of the NTF turns out to be almost constant in the signal band. In some cases, and particularly when the OSR is relatively low, this assumption may prove untrue, leading to a sub-optimal design.

c) In some design flows, the cut-off frequency of the NTF is used as a degree of freedom to satisfy the constraint $\|NTF\|_\infty < \gamma$. In some cases, particularly when γ is close to 1 or the OSR is low, this may result in some noise leaking into the signal band.

d) Most conventional design flows result in NTFs with steep transitions between the pass band and the stop band, particularly when the NTF is high order. This behavior is obviously inherent in the minimization of $\sigma_{\mathcal{B}}^2$. However, it may exacerbate the differences between the linearized and real modulator model. In turn, this may lead to inaccurate SNR predictions and in extreme cases to a lower robustness against instability.[1]

e) Many conventional design flows start with an LP modulator and obtain other modulator types (e.g. BP) via transformations. This makes it extremely hard if not impossible to cope with unusual modulator types (e.g., multi-band) that may be required by some applications.

IV. The Proposed NTF Optimization

In this Section, we mainly deal with point a) in the list above. Nonetheless, as a side effect, the proposed solution also addresses all the other points.

It is worth anticipating that our design strategy assumes and requires the NTF to be FIR. In practice, this is not a severe limitation. As a matter of fact, this choice is perfectly in line

[1]Even if we cannot provide a formal proof of this phenomenon, we have observed it in many of cases and it has intuitive explanations. We report one. If a modulator could be implemented *fully respecting* the specification of an extremely steep NTF (e.g., brick-wall), then violations of information theory principles could occur. In fact, one could recover the modulator input information *without any loss due to quantization* by using a brick-wall output filter, thus obtaining an information rate at the modulator output equal to that at the input. Since the latter can be arbitrarily large, this could imply an output information rate higher than the bit-rate, which is absurd. Thus, one can expect the conformance between the approximated linear model and the actual nonlinear model to deteriorate as the modulator is designed to have steeper NTFs, bringing in unexpected effects potentially including instability.

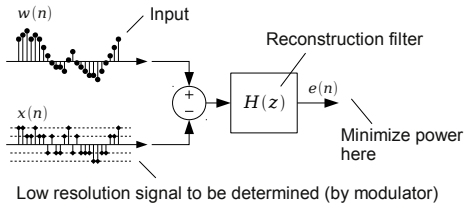

Figure 6. Interpretation of the modulator operation as the solution of an FA problem.

with the elementary, original high-order NTF form in Eqn. (6), where all the poles fall in the origin. With respect to this, we merely move the zeros. Consequently, our proposal can be seen as a strategy where only the NTF zeros are optimized. Lack of optimization for the poles means that results comparable to strategies which optimize the poles can only be achieved at a higher filter order. Indeed, this is the case. Yet, taking a higher filter order is not a problem since contrarily to conventional designs, we can synthesize high order NTFs (even 30-50 or more) without hindering the modulator stability. Furthermore, other FIR based strategies exist [17], also requiring large modulator orders.

A. Form to be optimized

As hinted in [13], [18], in order to deal with the output filter, one should interpret the $\Delta\Sigma$ modulator as a heuristic solver for an FA problem. Fig. 6 illustrates the problem nature. This consists in finding a discrete sequence $x(n)$ such that it is as similar as possible to a high-resolution or continuous valued input sequence $w(n)$, once passed through a filter $H(z)$. Clearly, $w(n)$ plays the role of the modulator input, $x(n)$ of the modulator output and $H(z)$ is the output filter. As shown in the figure, the concept of "similarity" can be formalized as a minimization of the average power at the output of the filter fed by $w(n) - x(n)$.

To solve the FA problem, the $\Delta\Sigma$ modulator rather than being designed after the minimization of $\sigma^2_{\mathcal{B}}$ in Eqn. (3) needs to be designed after the minimization of

$$\sigma^2_H = \int_0^\pi E(\omega) \left|NTF\left(\mathrm{e}^{\mathrm{i}\omega}\right)\right|^2 \left|H\left(\mathrm{e}^{\mathrm{i}\omega}\right)\right|^2 d\omega = \frac{\Delta^2}{12\pi} \int_0^\pi \left|NTF\left(\mathrm{e}^{\mathrm{i}\omega}\right)\right|^2 \left|H\left(\mathrm{e}^{\mathrm{i}\omega}\right)\right|^2 d\omega. \quad (8)$$

Let us assume that $NTF(z)$ is achieved by a P order FIR filter, with coefficients a_i, collectable in a vector $\boldsymbol{a} = (a_0, \ldots, a_P)^{\mathrm{T}}$. Namely,

$$NTF(z) = \sum_{k=0}^{P} a_k z^{-k}. \quad (9)$$

Let us also assume that $H(z)$ corresponds to a filter whose impulse response can safely be truncated to a finite number of samples collectable in a vector $\boldsymbol{h} = (h_0, \ldots, h_M)^{\mathrm{T}}$. Let us finally define $G(z) = NTF(z)H(z)$, so that the quantity object of minimization can be written as $\int_0^\pi \left|G(\mathrm{e}^{\mathrm{i}\omega})\right|^2 d\omega$. The impulse response corresponding to $G(z)$ can obviously be obtained as the convolution of a_i and h_i, as in

$$g_i = [a * h]_i = \sum_{j=-\infty}^{\infty} a_j \, h_{i-j} \quad (10)$$

where $*$ is the convolution operator and we take $a_i = 0$ for $i < 0$ or $i > P$ and $h_i = 0$ for $i < 0$ or $i > M$. Clearly, there are only a finite number of non-null entries in g_i, for $i = 0, \ldots, M + P$.

Eventually, recall the discrete form of Parseval's theorem, referred to $G(z)$

$$\frac{1}{2\pi} \int_{-\pi}^{\pi} \left|G(\mathrm{e}^{\mathrm{i}\omega})\right|^2 d\omega = \sum_{i=-\infty}^{\infty} |g_i|^2. \quad (11)$$

By substitution, neglecting all multiplicative constant terms, the quantity object of minimization can be expressed as

$$\sum_{i=0}^{M+P} \left(\sum_{j=0}^{P} a_j \, h_{i-j} \right)^2 \quad (12)$$

that can be further expanded into

$$\sum_{i=0}^{M+P} \sum_{j=0}^{P} \sum_{k=0}^{P} a_j \, a_k \, h_{i-j} \, h_{i-k}. \quad (13)$$

By swapping the sums, one gets

$$\sum_{j=0}^{P} \sum_{k=0}^{P} a_j \left(\sum_{i=0}^{M+P} h_{i-j} \, h_{i-k} \right) a_k. \quad (14)$$

that can be put in a more compact form exploiting a $(P+1) \times (P+1)$ matrix $\boldsymbol{Q}$ defined as

$$\boldsymbol{Q} = (q_{j,k}) \quad \text{where} \quad q_{j,k} = \sum_{i=0}^{M+P} h_{i-j} \, h_{i-k} \quad (15)$$

for $j, k \in \{0, \ldots, P\}$. With this, the form to be minimized becomes

$$\boldsymbol{a}^{\mathrm{T}} \, \boldsymbol{Q} \, \boldsymbol{a}. \quad (16)$$

Hence it is evident that one has a *quadratic optimization problem* defined over the filter coefficients. Clearly, $\boldsymbol{Q}$ must be positive semi-definite, since σ^2_H in (8) cannot be negative.

It is worth observing that in the definition of $\boldsymbol{Q}$ the summation can be extended to infinity as in

$$q_{j,k} = \sum_{i=-\infty}^{\infty} h_{i-j} \, h_{i-k} \quad (17)$$

to make evident that $\boldsymbol{Q}$ is Toeplitz [29] symmetric (it is in fact an auto-covariance matrix). This is interesting not just as a structural property, but also to reduce the computational burden of $\boldsymbol{Q}$ to the mere computation of its first row or first column. Focusing on the first row $q_{0,k} = \sum_{i=-\infty}^{\infty} h_i \, h_{i-k}$ one can also notice that to further reduce the computation burden the summation bounds can be restricted to $q_{0,k} = \sum_{i=k}^{M} h_i \, h_{i-k}$.

B. Application of the design constraints

The particular choice of a FIR structure for the NTF makes its stability (point 1 in Sec. III-A) and causality (point 2a) inherent. Thus, only two constraints remain: the need for a unitary first coefficient in the impulse response (point 4a); and the containment of $\|NTF\|_\infty$ (point 5, Lee criterion).

1) Unitary the first coefficient of the impulse response: thanks to the FIR nature of the NTF this merely requires fixing $\boldsymbol{a}_1 = a_0 = 1$. While this equality can be taken as a constraint for the minimization of (16), it is actually more convenient to use it to reduce the problem size. To this aim, observe that

$$\boldsymbol{a}^{\mathrm{T}}\,\boldsymbol{Q}\,\boldsymbol{a} = \begin{pmatrix}\boldsymbol{a}_1 & \boldsymbol{a}_{2:\bullet}^{\mathrm{T}}\end{pmatrix}\begin{pmatrix}\boldsymbol{Q}_{1,1} & \boldsymbol{Q}_{1,2:\bullet}\\ \boldsymbol{Q}_{2:\bullet,1} & \boldsymbol{Q}_{2:\bullet,2:\bullet}\end{pmatrix}\begin{pmatrix}\boldsymbol{a}_1\\ \boldsymbol{a}_{2:\bullet}\end{pmatrix} = a_0^2\,q_{0,0} + a_0\,\boldsymbol{a}_{2:\bullet}^{\mathrm{T}}\,\boldsymbol{Q}_{2:\bullet,1} + a_0\,\boldsymbol{Q}_{1,2:\bullet}\,\boldsymbol{a}_{2:\bullet} + \boldsymbol{a}_{2:\bullet}^{\mathrm{T}}\,\boldsymbol{Q}_{2:\bullet,2:\bullet}\,\boldsymbol{a}_{2:\bullet}. \quad (18)$$

Thanks to the symmetry of $\boldsymbol{Q}$, the two central entries can be rewritten as $2a_0\,\boldsymbol{Q}_{1,2:\bullet}\,\boldsymbol{a}_{2:\bullet}$. After the constantness of $q_{0,0}$ and thanks to $a_0 = 1$ the quantity object of minimization eventually reduces to

$$\boldsymbol{a}_{2:\bullet}^{\mathrm{T}}\,\boldsymbol{Q}_{2:\bullet,2:\bullet}\,\boldsymbol{a}_{2:\bullet} + 2\,\boldsymbol{Q}_{1,2:\bullet}\,\boldsymbol{a}_{2:\bullet}. \quad (19)$$

In other words, the constraint can be exploited for the reduction of the problem size at the mere cost of augmenting the minimization form by a linear term.

2) Lee criterion: Eqn. (2) represents an extremely complicated constraint. Indeed, it can be recast based on a *universal quantification*

$$\forall\omega \in [0,\pi] \quad \left|NTF\left(\mathrm{e}^{\mathrm{i}\omega}\right)\right| < \gamma \quad (20)$$

making evident that it summarizes an *infinitely large* set of inequalities in the frequency domain. Furthermore, the filter coefficients appear in $\left|NTF\left(\mathrm{e}^{\mathrm{i}\omega}\right)\right|$ in a nonlinear fashion.

Fortunately, the KYP lemma provides an extremely efficient way to convert universally quantified frequency domain inequalities of this sort into an alternative formulation based on the dual *existential quantifier*. This is extremely convenient since a minimization problem can often deal with existential quantifiers with the mere introduction of dummy variables. Furthermore, the KYP lemma gets the frequency domain inequality expressed through an arbitrary realization of a dynamical system providing the frequency domain behavior. This is also very convenient since it means that an inequality over the NTF can be directly expressed via the NTF coefficients.

From the KYP lemma, the following property holds.

Property 1 (Bounded real lemma)
If a transfer function $T(z)$ admits a state space representation $\mathcal{T}$ such that

$$\mathcal{T} = \left(\begin{array}{c|c}\boldsymbol{A} & \boldsymbol{B}\\ \hline \boldsymbol{C} & \boldsymbol{D}\end{array}\right)(z) \quad (21)$$

and $\mathcal{T}$ is stable and controllable, then an inequality such as

$$\|T\|_\infty \leq \gamma \quad (22)$$

can be recast in terms of the coefficients in $\boldsymbol{A}$, $\boldsymbol{B}$, $\boldsymbol{C}$ and $\boldsymbol{D}$ by asserting that

$$\exists \boldsymbol{P} \text{ square symmetric positive definite matrix such that } \begin{pmatrix}\boldsymbol{A}^{\mathrm{T}}\boldsymbol{P}\boldsymbol{A} - \boldsymbol{P} & \boldsymbol{A}^{\mathrm{T}}\boldsymbol{P}\boldsymbol{B} & \boldsymbol{C}^{\mathrm{T}}\\ \boldsymbol{B}^{\mathrm{T}}\boldsymbol{P}\boldsymbol{A} & \boldsymbol{B}^{\mathrm{T}}\boldsymbol{P}\boldsymbol{B} - \gamma^2 & \boldsymbol{D}\\ \boldsymbol{C} & \boldsymbol{D} & -1\end{pmatrix} \leq 0 \quad (23)$$

where the $\leq$ sign is here used to denote a generalized inequality stating negative semi-definiteness.

For an informal discussion of this property, see Appendix A.

Now, let $\mathcal{T}$ be a realization of the NTF such that

$$\left(\begin{array}{c|c}\boldsymbol{A} & \boldsymbol{B}\\ \hline \boldsymbol{C} & \boldsymbol{D}\end{array}\right)(z) = \left(\begin{array}{ccccc|c} 0 & 1 & 0 & \cdots & 0 & 0\\ 0 & 0 & 1 & \cdots & 0 & 0\\ \vdots & \vdots & \vdots & \ddots & \vdots & \vdots\\ 0 & 0 & 0 & \cdots & 1 & 0\\ 0 & 0 & 0 & \cdots & 0 & 1\\ \hline a_P & a_{P-1} & a_{P-2} & \cdots & a_1 & a_0\end{array}\right)(z). \quad (24)$$

This is a canonical realization, where $\boldsymbol{A}$ is responsible of making each state variable a delayed version of the preceding one, so that the state variables end up being a memory of the last P input samples [30]. Evidently, this realization is minimal (thus controllable) and only $\boldsymbol{C}$ depends on the filter coefficients that are object of optimization. Hence, the left hand side of inequality (23) is affine in the coefficients object of minimization. Furthermore, it is *affine* in the entries of $\boldsymbol{P}$. Hence, collecting in a vector $\boldsymbol{\xi}$ all the filter coefficients $a_1,\ldots,a_P$ and all the independent entries in $\boldsymbol{P}$ to get an L entry vector $(\xi_1,\ldots\xi_L)^{\mathrm{T}}$, it must be that (23) can be expressed as $\boldsymbol{M}(\boldsymbol{\xi}) \leq 0$ with

$$\boldsymbol{M}(\boldsymbol{\xi}) = \boldsymbol{M}_0 + \sum_{i=1}^{L}\boldsymbol{M}_i\,\xi_i \quad (25)$$

where $\boldsymbol{M}_0,\ldots\boldsymbol{M}_L$ are symmetric matrices. Regardless of the entries of the $\boldsymbol{M}_i$ matrices (that are unimportant here), this shows that (23) is a Linear Matrix Inequality (LMI). Such property is quite important, as it states that (23) is a convex constraint.

C. Summary of the optimization problem

It is now possible to summarize the optimization problem. To find P filter coefficients $a_1,\ldots,a_P$, one needs to build a problem with L variables $\xi_1,\ldots,\xi_L$. The first P of them are the filter coefficients themselves, while the last $L-P$ are entries of matrix $\boldsymbol{P}$, functional to the solution of the problem, but uninteresting and due to be eventually discarded.

The problem consists in the minimization of the convex quadratic form in Eqn. (19), which is also a convex quadratic form in $\boldsymbol{\xi}$. One has the constraint $\boldsymbol{P} > 0$, which is an LMI in $\boldsymbol{\xi}$ and the constraint in Eqn. (23), which has just been shown to be an LMI in $\boldsymbol{\xi}$. Altogether, one has a problem that can be tackled

by SDP. In recent times, *interior point methods* [22], [31] allow problems of this sort to be solved in polynomial time with respect to the problem size. On commodity hardware, problems with a thousand of variables or more can be solved in a few seconds. In our case the number of variables is dominated by the number of independent entries in $\boldsymbol{P}$, which is $P \times P$. Since $\boldsymbol{P}$ is symmetric, this means having ${}^{P}/_{2} \cdot (P+1)$ independent entries and ${}^{P}/_{2} \cdot (P+2)$ variables overall. Consequently, one can easily go up to filter orders of 50 or more. In practice, as Section V shows, there is hardly a need to reach such high orders. That section provides practical examples obtained with an SDP code distributed under a free, open source licence, proving that tackling our optimization problem is not just possible, but also quite affordable.

D. Positive side effects of the proposed optimization

After having illustrated how the proposed NTF optimization deals with issue a) in Sec. III-C, it is worth considering also the other items. Points b) and c) are automatically eliminated thanks to the different design strategy. Particularly, the proposed methodology is completely agnostic of the OSR. With respect to point d), our strategy tends to provide NTFs that are *only as steep as needed* and typically just as steep as the reconstruction filter is. Eventually, with respect to point e), our strategy can deal with any kind of modulator, even the most unusual one, with no need for frequency transformations. For instance, a multi-band modulator will obviously have a multi-band output filter. Feeding such filter into the our design procedure, automatically leads to the required NTF.

V. Design examples and comparison to conventional design flows

The design examples proposed in this Section have been tested by coding our strategy in the Python programming language taking advantage of the Numpy and Scipy packages [32]. Python is a modern general purpose programming language renown for its conciseness and extensibility. Numpy and Scipy expand it into a powerful, matrix-oriented numerical computing environment that can be freely deployed on all major computing platforms. SDP has been addressed using a further Python module, the CVXOPT free software package for convex optimization [33]. Specifically, CVXOPT has been used as a backend solver, while the CVXPY package [34] has been employed as a modeling framework to express the optimization problem in a more natural form under the rules of Disciplined Convex Programming (DCP) [35]. Comparison to conventional $\Delta\Sigma$ modulator design flows has been practiced by the DELSIG toolbox [16] and the code provided with [17]. DELSIG has also been used for the time domain simulation of the modulators. A sample of our code is available. Please refer to Appendix B for information on how to obtain it.

A. LP modulator with first order output filter

The first design case regards a binary LP modulator, targeting signal synthesis and coupled with a 1st order reconstruction filter. The signal band extends from dc to 1 kHz and the OSR is 1024 (i.e., the modulator operates at approximately 2 MHz). To avoid spurious attenuation at the filter output, the reconstruction filter is designed with its cut-off frequency set at 2 kHz. The Lee coefficient γ is set at 1.5. Fig. 7 shows the output filter profile and the NTFs obtained with the `synthesizeNTF` function in DELSIG (for a 4th order modulator with optimized zeros) and our approach (for a 12th order FIR NTF).[2]

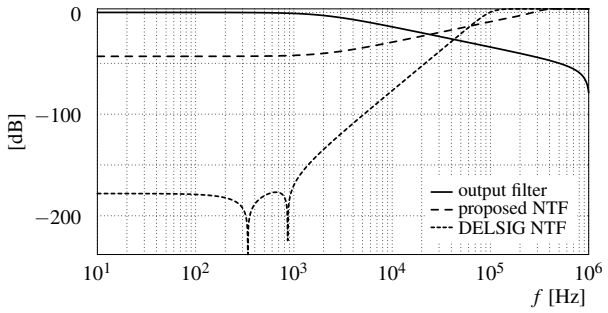

Figure 7. Output filter, proposed NTF and NTF obtained by a conventional design flow, for the test case in Section V-A.

The choice of a 12th order for the proposed strategy is not casual. As a matter of fact, in the proposed approach the performance improves (i.e., σ_H reduces) as the order is increased. However, the improvement is initially very rapid, then it slows down. This is well evident in figure 8, which shows the convergence to the optimal NTF shape. For orders higher than 6, the NTF shape is almost invariant. Clearly, it is convenient to stop increasing the order as soon as σ_H levels off, which happens slightly above 10. Interestingly, a similar convergence is not experienced in other design strategies, which keep delivering different (and improved, according to their merit factors) NTFs as the order is increased, so that the limit is the loss of robust behavior or the loss of numerical accuracy in the optimizer. Incidentally, this is the reason why we can compare modulators having different orders. Indeed, we compare the best modulator designed with the proposed strategy to modulators designed with other strategies at a reasonable trade-off between quality and robustness.

Interestingly, the NTF obtained by our design flow turns out to be by far less aggressive than the conventional one, exhibiting a much lower attenuation in the signal band. Nonetheless, its performance is better. An estimation of the output SNR, for an input sinusoid with amplitude $A = 0.4$ (normalized to the quantization levels set at ± 1) can be obtained as

$$SNR_{\text{expected}} = \frac{A^2}{2\sigma_H^2} \tag{26}$$

and gives 42.9 dB for the proposed approach and 38.4 dB for the conventional (`synthesizeNTF`) NTF with a difference over 4.5 dB. Computing the SNR by time domain simulation (that let one use the actual nonlinear modulator model) returns 42.4 dB for the proposed technique and 40.3 dB for the conventional one, so that the advantage reduces to about 2 dB, still being well perceivable. The SNR numbers have been obtained by

[2]We tried to compare also to the method in [17], but the provided code seems to run into numerical stability problems for this very large OSR.

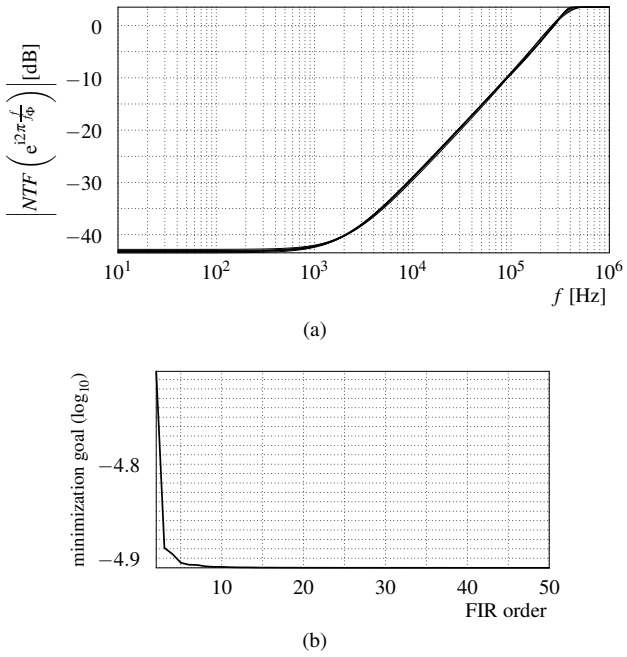

Figure 8. Convergence of the NTF to its optimal shape for increasing filter orders $5, 6, 9, 13, 18, 25$ (a) and improvement in minimization goal as the FIR order is increased (b). In (a), the six curves superimpose almost perfectly. Data for the test case in Section V-A.

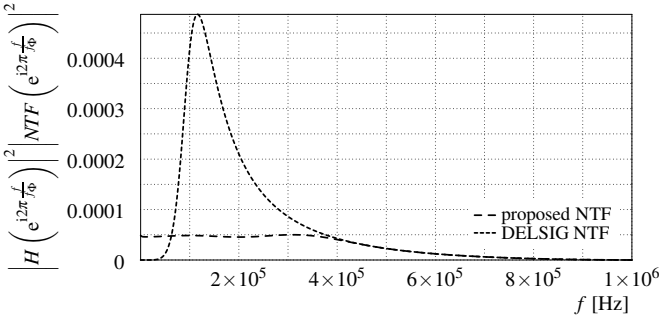

Figure 9. Integrand appearing in the definition of σ_H^2 for the proposed NTF and the NTFs obtained by a conventional design flow. Data for the test case in Section V-A.

replicating in software the architecture in Fig. 6. Excited with the modulator input alone as $w(n)$, it lets one measure the signal power at $e(n)$, while excited with both the modulator input at $w(n)$ and output at $x(n)$ it lets one measure the noise power at $e(n)$.

A justification for the apparent paradox of having a better behavior with a less aggressive NTF comes from Fig. 9, which shows $\left|H\left(e^{i\omega}\right)\right|^2\left|NTF\left(e^{i\omega}\right)\right|^2$ in the three cases. Here, thanks to the linear scale, it is well evident that the advantage of the conventional NTFs within the signal band is more than compensated by the advantage of the proposed NTF out of it.

It is even more interesting to note that a ΔΣ modulator based on the proposed NTF can behave much more robustly than a conventional one. Even with large input signals, it can operate correctly, without overloading its quantizer. Conversely, the 4th order modulator obtained by the `synthesizeNTF` design flow is much more fragile due to its steepness. For instance, at

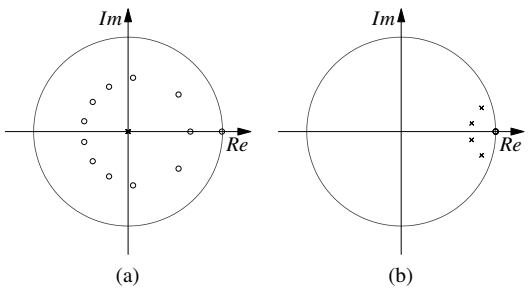

Figure 10. Comparison of pole-zero placement for the proposed design strategy (a) and a conventional ones, namely `synthesizeNTF` from DELSIG (b). Data from the test case in Section V-A.

a signal amplitude $A = 0.7$ it already breaks, unless the Lee coefficient γ is lowered to 1.4. Conversely, the proposed NTF makes the modulator work correctly up to $A = 1$. Furthermore, for A values in little excess of 1 where *by definition* the modulator is not meant to operate, one initially sees a graceful degradation of performance, rather than a full breakage. For instance at $A = 1.1$ one sees the SNR reducing to 30 dB. The other way round, this increased robustness can be used to bring the Lee coefficients to higher values without breaking the modulator operation, cashing a further little advantage in terms of SNR. For instance, for the output filter under exam, the proposed design technique lets a modulator be designed with $\gamma = 2$ gaining 1 further dB in SNR. As a matter of fact, we have verified that even $\gamma = 4$ is tolerated, although without any SNR advantage.

Intuitively, the increased robustness is a consequence of the fact that the proposed technique makes the NTF no steeper than it is really needed, matching the steepness of the output filter. Incidentally, this explains the convergence in 8. Once the required steepness is reached, there is no need to rise the order any further.

Fig. 10 compares our pole/zero positioning to conventional ones.

A final remark can be dedicated to the computational resources needed by the optimization. For FIR order $P = 12$, a business laptop computer with a Core 2 Duo (Penryn, 2009) CPU and 4 GB of RAM shared with the video card, can perform the SDP almost instantaneously.

B. BP modulator with output filter with steep features

The second test case regards again a binary modulator, this time for BP signals. The signal band is centered at 1 kHz and extends for 400 Hz. The OSR is set at 64. This time, the output filter is much steeper than in the previous example, consisting in an 8th order Butterworth filter. The Lee coefficient γ is set at 1.5. Fig. 11 shows the output filter profile and the NTFs obtained with: the `synthesizeNTF` function in DELSIG (for a 4th order modulator with optimized zeros); the method in [17] (for a 49th order modulator); and our approach (for a 49th order FIR NTF).

In this case, the higher roll-off of the output filter requires a higher NTF order for our methodology, as evident for the convergence analysis in Fig. 12. From the second plot, a 32th

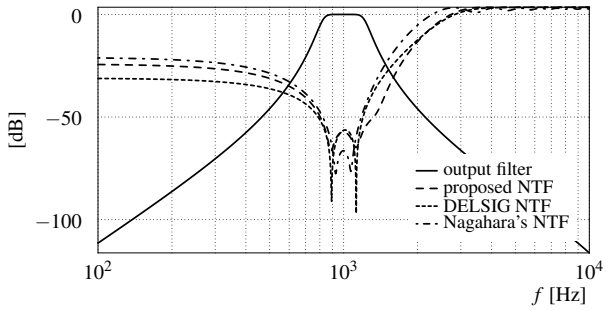

Figure 11. Output filter, proposed NTF and NTFs obtained by two conventional design flow, for the test case in Section V-B.

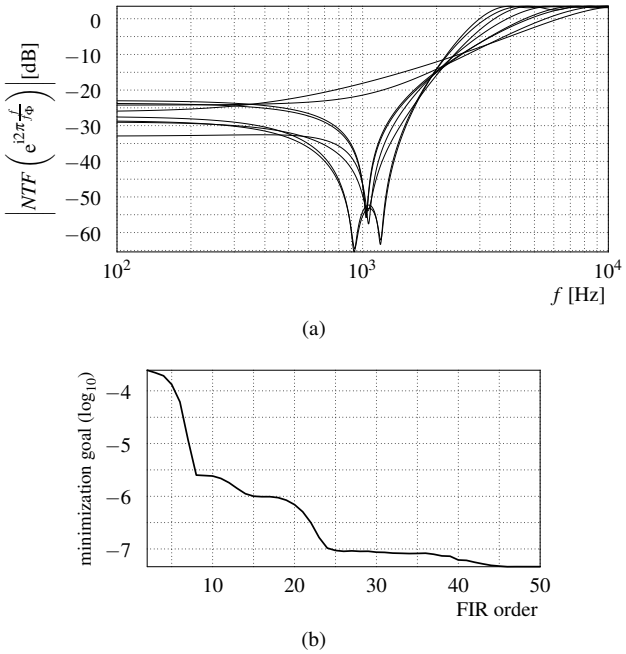

Figure 12. Convergence of the NTF to its optimal shape for increasing filter orders $5, 8, 11, 15, 21, 28, 37, 49$ (a) and improvement in minimization goal as the FIR order is increased (b). In (a), the last 2 curves superimpose almost perfectly. Data for the test case in Section V-B.

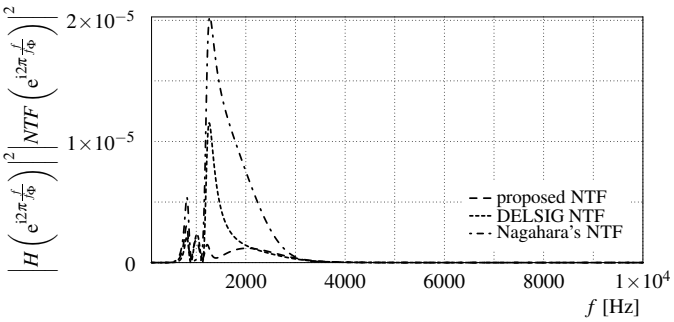

Figure 13. Integrand appearing in the definition of σ_H^2 for the proposed NTF and the NTFs obtained by two conventional design flows. Data for the test case in Section V-B.

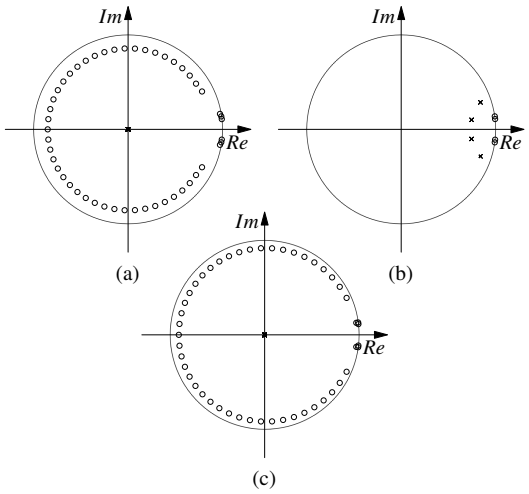

Figure 14. Comparison of pole-zero placement for the proposed design strategy (a) and two conventional ones, namely `synthesizeNTF` from DELSIG (b) and Nagahara's strategy in [17] (c). Data from the test case in Section V-B.

order NTF would already give good results. Note that the 49th order FIR takes a couple of minutes to compute via SDP on the same laptop used for the previous test case.

As for the previous test case, it is interesting to observe the integrand appearing in the definition of σ_H^2. This is plotted in Fig. 13.

In this case, for a sinusoidal input with $A = 0.75$ we get an SNR (from time domain simulation) after the output filter of 69.2 dB for our design approach, 67.0 dB for the `synthesizeNTF` design flow, and 68.1 dB for the method in [17]. Note that trying to pick a 6th order NTF with the `synthesizeNTF` design flow would lead to a misbehaving modulator, while our approach enables increasing the FIR order even above 49.

Fig. 14 compares our pole/zero positioning to the conventional ones for this test case.

This test case shows that the advantage of the proposed approach may fade a little when the output filter has steep cutoff characteristics close to an ideal on-off behavior. This is quite reasonable, since an on-off filter behavior is exactly the premise on which conventional design flows are funded. Yet, even in this case some advantages remain evident, including those in terms of SNR.

C. Multi-band modulator

The last case that we consider is that of a multi-band modulator. This is intractable in many conventional design flows [16], although it can be managed by the recent methodology in [17].[3] Assume that the input signal has two bands, one centered at 1 kHz and 400 Hz wide and the other centered at 10 kHz and 4 kHz wide. Let the OSR be 64 (i.e., $f_\Phi = 2\cdot64\cdot(4000+400)$ Hz). Consider the case of a 2-band 8th order Butterworth filter at the output. As usual, for the modulator design consider the binary case, with $\gamma = 1.5$. Fig. 11 shows the

[3]Note that the method in [17] targets a slightly different goal for the single and the multi-band case. Furthermore, it requires a new matrix inequality for each band so that it can become increasingly demanding in terms of computational power when their number is increased. Finally, the sample code delivered with the paper cannot deal with cases where the signal bands have different widths, although it can be easily extended for it.

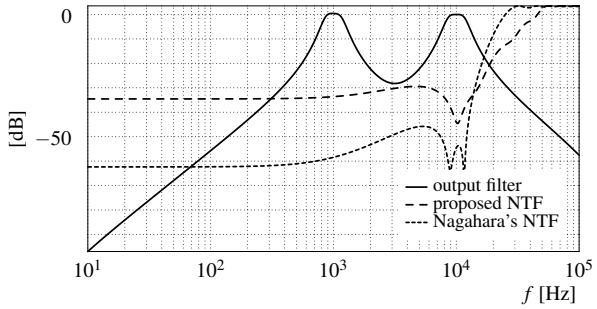

Figure 15. Output filter, proposed NTF, and conventional NTF synthesized by the method in [17] for the test case in Section V-C.

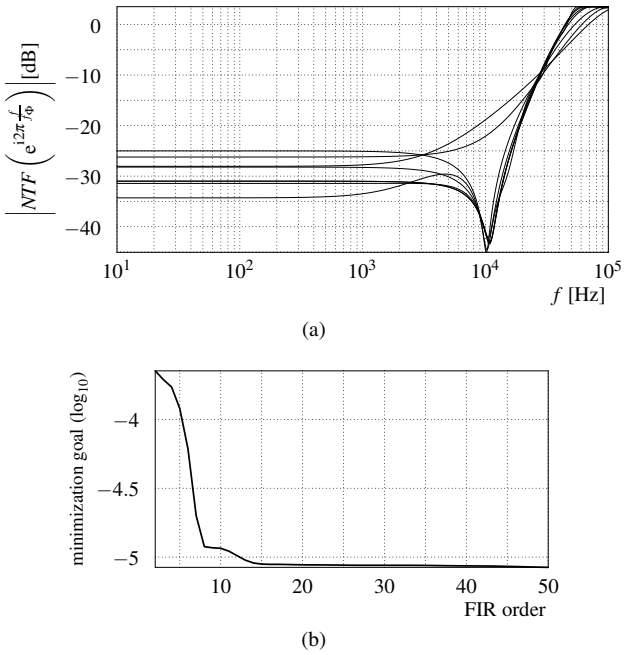

Figure 16. Convergence of the NTF to its optimal shape for increasing filter orders $5, 8, 11, 15, 21, 28, 37, 49$ (a) and improvement in minimization goal as the FIR order is increased (b). In (a), the last 3 curves superimpose very well. Data for the test case in Section V-C.

output filter profile and the NTFs obtained with in our approach (for a 50$^{\text{th}}$ order FIR NTF). Obviously, it is not possible to design an NTF for this case using `synthesizeNTF`, so we provide comparison only to the the method in [17] for the same FIR order.

As for the previous test cases, Fig. 16 shows the NTF convergence to the optimal shape as the FIR order P is increased. Evidently, FIR orders of 16 would already be enough to achieve a good SNR.

In this case, simulating the modulator for an input signal given by the superposition of two tones at 1 and 10 kHz, with amplitude $A = 0.45$ for both of them, gives an SNR of over 46 dB at the filter output. The modulator based on the method in [17] is unstable at this large input. At $A = 0.40$ it operates correctly, though, and it can be taken as a reference. In this condition, our method delivers a 48.2 dB SNR, vs a 42.3 dB SNR for the reference algorithm, namely we have an almost 6 dB advantage. This large advantage should be no surprise,

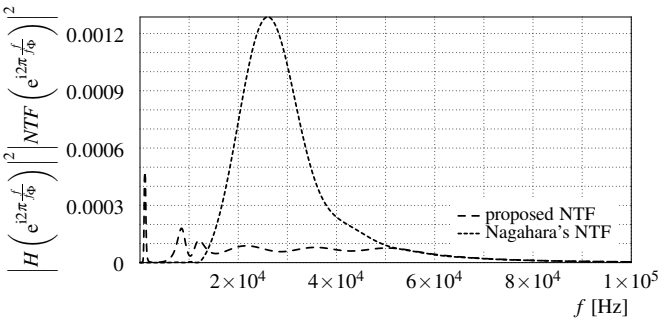

Figure 17. Integrand appearing in the definition of σ_H^2 for the proposed NTF and a conventional NTF designed following the method in [17]. Data for the test case in Section V-C.

since we explicitly optimize for the SNR on the filtered output, while [17] uses a different merit factor.

What is interesting about this multi-band case is that it shows a rather counter-intuitive behaviour. Looking at the input signal structure, one would probably think that the modulator should put its quantization noise in 3 regions: at low frequencies, before the first signal band, at intermediate frequencies, between the signal bands and at high frequencies, above the second signal band. Furthermore, one would think that the modulator should have zones of very high attenuation for the noise in the two signal bands. Conversely, our design approach shows that it is more convenient to use all the available degrees of freedom on the NTF to optimize the noise shaping at the high frequencies, completely ignoring the two lower bands that are anyway extremely thin and thus incapable to contain much noise. Additionally, it shows that it would be a waste to strive to remove too much noise from the first signal band, that is anyway very thin and thus incapable to contribute much to the overall SNR. This is very well evident from the graph in Fig. 17 which shows $\left|H\left(e^{i\omega}\right)\right|^2\left|NTF\left(e^{i\omega}\right)\right|^2$, namely the integrand in the expression of σ_H^2, both for our NTF and the one obtained following [17]. Thanks to the linear scale, it is apparent that it is much more important to practice a good noise allocation at the high frequencies above 12 kHz than in the thin bands between dc and 800 Hz and between 1200 and 8000 Hz. Furthermore, it is interesting to look at the first peak in the plot. This is due to the fact that the NTF attenuates much less in the first signal band than in the second. However, the linear scale makes this peak appear as it really is: so thin that its *mass* and thus its contribution to the overall SNR is anyway very modest. Indeed, the NTF based on [17], that strives to remove a lot of noise also from the first signal band, lacks this peak, but pays it with a much higher integrand right above the second band.

Finally, Fig. 18 shows the pole-zero location, which is somehow similar to that in Fig. 14, given that also in this case we end up with a BS NTF.

VI. Conclusions

In this paper we have proposed a new design flow for ΔΣ modulators. Contrarily to conventional strategies, our methodology is aware of the output filter that in most practical

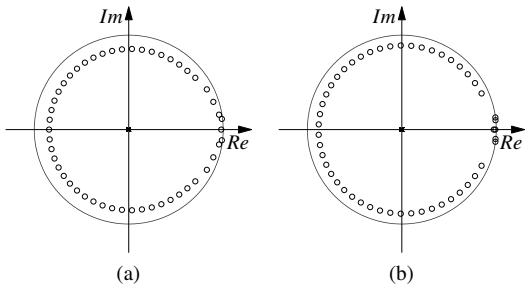

Figure 18. Pole-zero placement for the proposed design strategy (a) and the conventional one in [17] (b) for the test case in Section V-C.

applications is placed at the modulator output. This is an important difference, since common strategies assume that an ideal filter is available, with a steep on-off behavior between the signal band and the noise band. Consequently, they only strive at putting most of the noise out of the signal band. Conversely, our strategy strives to shape the quantization noise so that the overall noise after the output filter can be minimized.

In practice the two approaches may become similar when a steep filter is indeed available. Yet, they significantly differ when one can only count on a filter with a non-ideal roll-off. In this latter case, our strategy consistently provides a better behavior. It is worth underlining that this situation emerges in a large number of applications. Specifically, whenever one uses $\Delta\Sigma$ modulation for signal synthesis, power conversion or actuation, the output filter is analog and often lacks aggressive specifications. As a matter of fact, when one talks about actuation (ac motor drives, audio amplification), it frequently happens that the filter is realized taking advantage of the actuator input impedance. In this case, the filter designer may get quite confined in his choices. Extensive simulations (some of which presented in the paper) have shown evident SNR improvements in cases where the modulator works in conjunction with not-so-good output filters. However, even when output filters with a good roll-off are available there might be minor SNR increases.

Another distinguished advantage of the proposed approach is that it does never lead to a NTF that is steeper than it is strictly needed. This helps keeping the modulator stable and resilient to input conditions that could otherwise undermine its behavior (e.g., too large input signals).

Finally, the proposed methodology lets one tackle design cases that are often unmanageable by conventional flows. As an example, we have proposed the case of a modulator for multi-band signals.

The approach that we have described is based on the KYP lemma and obtains the NTF through an optimization process exploiting SDP. The resulting NTFs are in the FIR class. Current day algorithms enable a very rapid design process even for high-order modulators. Typical computation times may be between a few seconds to a few minutes even on a standard laptop. In practice, our simulations show that, in most cases, FIR orders can be kept relatively low.

As a final remark, note that being based on a formal process, our strategy can return truly optimal NTF shapes. Interestingly, there are cases when these may at first appear counter-intuitive so that only a more thorough exam lets one see a justification.

APPENDIX

A. Discussion about the bounded real lemma

Here, we provide an informal discussion of Property 1. The interested reader is invited to refer to [36] for formal considerations.

The so called KYP lemma actually refers to a loosely defined set of theorems related to dissipation inequalities. Restricting to discrete time models, consider a system $\mathcal{T}$ with n state variables $\boldsymbol{x}$, m inputs $\boldsymbol{u}$ and p outputs $\boldsymbol{y}$

$$\mathcal{T} = \left(\begin{array}{c|c} \boldsymbol{A} & \boldsymbol{B} \\ \hline \boldsymbol{C} & \boldsymbol{D} \end{array}\right)(z) \tag{27}$$

The system is said to be dissipative with respect to a real valued supply rate $s(\boldsymbol{x},\boldsymbol{u})$ if there exists a continuous real valued function $V(\boldsymbol{x})$, named storage function, such that the dissipation inequality

$$V(\boldsymbol{x}(n+1)) - V(\boldsymbol{x}(n)) \leq s(\boldsymbol{x}(n),\boldsymbol{u}(n)) \tag{28}$$

holds for all the admissible $\boldsymbol{x}$, $\boldsymbol{u}$ trajectories. Clearly, the storage function can be seen as a generalization of the energy accumulated by the system, while the supply rate can be seen as a generalization of the rate at which energy is provided to or taken from it.

For practical systems, it is reasonable to assume that the rate function is a quadratic form on $\boldsymbol{x}$ and $\boldsymbol{u}$, as in

$$s(\boldsymbol{x},\boldsymbol{u}) = \begin{pmatrix}\boldsymbol{x}\\ \boldsymbol{u}\end{pmatrix}^{\mathrm{T}} \hat{\boldsymbol{Q}} \begin{pmatrix}\boldsymbol{x}\\ \boldsymbol{u}\end{pmatrix} \tag{29}$$

where $\hat{\boldsymbol{Q}}$ is a symmetric real matrix.

A first part of the KYP lemma establishes that for a linear system with a quadratic supply rate the dissipation inequality can be satisfied for some continuous storage function $V(\boldsymbol{x})$ if and only if it is satisfied for some *quadratic* storage function $V(\boldsymbol{x}) = \boldsymbol{x}^{\mathrm{T}}\boldsymbol{P}\boldsymbol{x}$ where $\boldsymbol{P}$ is real symmetric. In this case, the dissipation inequality can be expressed as

$$(\boldsymbol{A}\boldsymbol{x}+\boldsymbol{B}\boldsymbol{u})^{\mathrm{T}}\,\boldsymbol{P}\,(\boldsymbol{A}\boldsymbol{x}+\boldsymbol{B}\boldsymbol{u}) - \boldsymbol{x}^{\mathrm{T}}\,\boldsymbol{P}\,\boldsymbol{x} \leq s(\boldsymbol{x},\boldsymbol{u}) \tag{30}$$

This can be equivalently recast as

$$\begin{pmatrix}\boldsymbol{x}\\ \boldsymbol{u}\end{pmatrix}^{\mathrm{T}} \begin{pmatrix}\boldsymbol{A}^{\mathrm{T}}\boldsymbol{P}\boldsymbol{A}-\boldsymbol{P} & \boldsymbol{A}^{\mathrm{T}}\boldsymbol{P}\boldsymbol{B}\\ \boldsymbol{B}^{\mathrm{T}}\boldsymbol{P}\boldsymbol{A} & \boldsymbol{B}^{\mathrm{T}}\boldsymbol{P}\boldsymbol{B}\end{pmatrix} \begin{pmatrix}\boldsymbol{x}\\ \boldsymbol{u}\end{pmatrix} \leq \begin{pmatrix}\boldsymbol{x}\\ \boldsymbol{u}\end{pmatrix}^{\mathrm{T}} \hat{\boldsymbol{Q}} \begin{pmatrix}\boldsymbol{x}\\ \boldsymbol{u}\end{pmatrix} \tag{31}$$

Eventually, since the inequality should hold for all $\boldsymbol{x}$ and $\boldsymbol{u}$ one has

$$\begin{pmatrix}\boldsymbol{A}^{\mathrm{T}}\boldsymbol{P}\boldsymbol{A}-\boldsymbol{P} & \boldsymbol{A}^{\mathrm{T}}\boldsymbol{P}\boldsymbol{B}\\ \boldsymbol{B}^{\mathrm{T}}\boldsymbol{P}\boldsymbol{A} & \boldsymbol{B}^{\mathrm{T}}\boldsymbol{P}\boldsymbol{B}\end{pmatrix} - \hat{\boldsymbol{Q}} \leq 0 \tag{32}$$

which should be intended as a generalized matrix inequality imposing negative semi-definiteness. Furthermore, posing a

positive definiteness restriction on $V(\boldsymbol{x})$ requires and is implied by $\boldsymbol{P}$ being positive semi-definite.

A second part in the lemma establishes that while originally conceived for real state and input vector $\boldsymbol{x}$ and $\boldsymbol{u}$, it can be extended to complex vectors $\boldsymbol{X}$ and $\boldsymbol{U}$. With this, Eqn. (29) becomes a *Hermitian* form. Interestingly, by taking $\boldsymbol{X}$ and $\boldsymbol{U}$ so that model (27) is valid in the z-domain and restricting to $z \in \mathbb{C}$ such that $|z| = 1$ (i.e., to sinusoidal regime with $\omega \in [-\pi, \pi]$ and $z = \mathrm{e}^{\mathrm{i}\omega}$), the inequality (30) compells the Hermitian form to be positive. Most notably, the *frequency domain inequality* version of the KYP states that the inverse also holds. Namely, the positive semi-definiteness of $s(\boldsymbol{X}, \boldsymbol{U})$ with complex variables and $z = \mathrm{e}^{\mathrm{i}\omega}$ requires the existence of a positive semi definite real symmetric $\boldsymbol{P}$ satisfying (32). Actually, for this part of the lemma to hold an additional assumption of controllability on $\mathcal{T}$ is required.

Let us now take m and p equal to 1 and assume that

$$s(\boldsymbol{X}, U) = \gamma |U|^2 - |\boldsymbol{C}\boldsymbol{X} + \boldsymbol{D}U|^2 \tag{33}$$

Restricting to the unit circle in the z plane, the positive semi-definiteness of such an $s(\cdot)$ means that at any frequency ω the power of $y = \boldsymbol{C}\boldsymbol{x} + \boldsymbol{D}u$ is less than γ^2 times the power of u, namely that the input-output gain of the system is less than γ. In other words, if $T(z)$ is the transfer function between u and y, one has $\|T\|_\infty \leq \gamma$.

The Hermitian form associated to Eqn. (33) needs

$$\hat{\boldsymbol{Q}} = \begin{pmatrix} -\boldsymbol{C}^{\mathrm{T}}\boldsymbol{C} & -\boldsymbol{C}^{\mathrm{T}}\boldsymbol{D} \\ -\boldsymbol{D}^{\mathrm{T}}\boldsymbol{C} & -\boldsymbol{D}^{\mathrm{T}}\boldsymbol{D} + \gamma^2 \end{pmatrix} \tag{34}$$

Substituting it into (32) gives

$$\begin{pmatrix} \boldsymbol{A}^{\mathrm{T}}\boldsymbol{P}\boldsymbol{A} - \boldsymbol{P} + \boldsymbol{C}^{\mathrm{T}}\boldsymbol{C} & \boldsymbol{A}^{\mathrm{T}}\boldsymbol{P}\boldsymbol{B} + \boldsymbol{C}^{\mathrm{T}}\boldsymbol{D} \\ \boldsymbol{B}^{\mathrm{T}}\boldsymbol{P}\boldsymbol{A} + \boldsymbol{D}^{\mathrm{T}}\boldsymbol{C} & \boldsymbol{B}^{\mathrm{T}}\boldsymbol{P}\boldsymbol{B} - \gamma^2 + \boldsymbol{D}^{\mathrm{T}}\boldsymbol{D} \end{pmatrix} \leq 0 \tag{35}$$

Let us now look at the matrix

$$\begin{pmatrix} \boldsymbol{A}^{\mathrm{T}}\,\boldsymbol{P}\,\boldsymbol{A} - \boldsymbol{P} & \boldsymbol{A}^{\mathrm{T}}\,\boldsymbol{P}\,\boldsymbol{B} & \boldsymbol{C}^{\mathrm{T}} \\ \boldsymbol{B}^{\mathrm{T}}\,\boldsymbol{P}\,\boldsymbol{A} & \boldsymbol{B}^{\mathrm{T}}\,\boldsymbol{P}\,\boldsymbol{B} - \gamma^2 & \boldsymbol{D} \\ \boldsymbol{C} & \boldsymbol{D} & -1 \end{pmatrix}. \tag{36}$$

Evidently, the matrix in (35) is the *Schur's complement* of the bottom right sub-matrix (-1) in matrix (36). Eventually, recall the Schur's complement conditions for positive (negative) definiteness [37]. These basically state that a matrix $\boldsymbol{M}$ is positive (negative) semi-definite if and only if the Schur's complement $\boldsymbol{S}$ of a sub-matrix $\boldsymbol{S}_M$ in $\boldsymbol{M}$ is positive (negative) semi-definite and $\boldsymbol{S}_M$ is positive (negative) definite. This implies that being -1 a negative scalar, the inequality (35) holds if and only if the matrix in (36) is negative semi-definite.

B. Sample code for the proposed design method

Sample code for the proposed ΔΣ Modulator design flow can be downloaded at the following site http://pydsm.googlecode.com. The code is licensed under a free, open-source license. Please follow the instructions in the `README` to install the software and all the dependencies necessary for its usage. The `README` also contains some information on how to replicate the examples proposed in this paper. In case you find this software useful, please propagate information about this paper which constitutes a fundamental part of its documentation.

REFERENCES

[1] S. R. Norsworthy, R. Schreier, and G. C. Temes, Eds., *Delta-Sigma Data Converters: Theory, Design, and Simulation*. Wiley-IEEE Press, 1996.

[2] J. D. Reiss, "Understanting Sigma-Delta modulation: The solved and unsolved issues," *Journal of Audio Engineering Soc.*, vol. 56, no. 1+2, pp. 49–64, Feb. 2008.

[3] R. Schreier and G. C. Temes, *Understanding Delta-Sigma Data Converters*. Wiley-IEEE Press, 2004.

[4] J. M. de la Rosa, "Sigma-Delta modulators: Tutorial overview, design guide, and state-of-the-art survey," *IEEE Trans. Circuits Syst. I*, vol. 58, no. 1, pp. 1–21, Jan. 2011.

[5] D. Reefman and E. Janssen, "Signal processing for direct stream digital: A tutorial for digital Sigma-Delta modulation and 1-bit digital audio processing," Philips Research Eindhoven, White Paper 18, Dec. 2002.

[6] D. Yang, F. F. Dai, W. Ni, S. Yin, and R. C. Jaeger, "Delta-Sigma modulation for direct digital frequency synthesis," *IEEE Trans. VLSI Syst.*, vol. 17, no. 6, pp. 793–802, Jun. 2009.

[7] E. Gaalaas, "Class D audio amplifiers: What, why, and how," *Analog Dialogue*, vol. 40, no. 6, pp. 1–7, Jun. 2006.

[8] F. M. Ghannouchi, "Power amplifier and transmitter architectures for software defined radio systems," *IEEE Circuits Syst. Mag.*, no. 4, pp. 56–63, 2010.

[9] E. Dallago and G. Sassone, "Advances in high-frequency power conversion by Delta–Sigma modulation," *IEEE Trans. Circuits Syst. I*, vol. 44, no. 8, pp. 712–721, Aug. 1997.

[10] B. Jacob and M. R. Baiju, "Vector quantized space vector based spread spectrum modulation scheme for multilevel inverters using the principle of oversampling ADC," *IEEE Trans. Ind. Electron.*, to appear in 2012.

[11] I. Galton, "Delta–Sigma data conversion in wireless transceivers," *IEEE Trans. Microw. Theory Tech.*, vol. 50, no. 1, pp. 302–315, Jan. 2002.

[12] Y. Dong, M. Kraft, and W. Redman-White, "Micromachined vibratory gyroscopes controlled by a high-order bandpass Sigma-Delta modulator," *IEEE Sensors J.*, vol. 7, no. 1, pp. 59–69, Jan. 2007.

[13] S. Callegari, F. Bizzarri, R. Rovatti, and G. Setti, "On the approximate solution of a class of large discrete quadratic programming problems by ΔΣ modulation: the case of circulant quadratic forms," *IEEE Trans. Signal Process.*, vol. 58, no. 12, pp. 6126–6139, Dec. 2010.

[14] F. Bizzarri and S. Callegari, "A heuristic solution to the optimisation of flutter control in compression systems (and to some more binary quadratic programming problems) via ΔΣ modulation circuits," in *Proc. of ISCAS'10*, Paris, FR, May 2010.

[15] F. Bizzarri, C. Buchheim, S. Callegari, A. Caprara, A. Lodi, R. Rovatti, and G. Setti, "Practical solution of periodic filtered approximation as a convex quadratic integer program," in *Complex Systems Design and Management, Procedings of the First International Confernce on. CSDM 2010*. Paris: Springer, Oct. 2010, pp. 149–160.

[16] R. Schreier, *The Delta-Sigma Toolbox*, Analog Devices, 2011, release 7.4, also known as "DELSIG". [Online]. Available: http://www.mathworks.com/matlabcentral/fileexchange/

[17] M. Nagahara and Y. Yamamoto, "Frequency domain Min-Max optimization of noise-shaping Delta-Sigma modulators," *IEEE Trans. Signal Process.*, vol. 60, no. 6, pp. 2828–2839, Jun. 2012.

[18] F. Bizzarri, S. Callegari, R. Rovatti, and G. Setti, "On the synthesis of periodic signals by discrete pulse-trains and optimisation techniques," in *Proc. of ECCTD'09*, Antalya (TR), Aug. 2009, pp. 584–587.

[19] *LM4670 Filterless High Efficiency 3W Switching Audio Amplifier*, Texas Instruments, Jun. 2006, TI Literature Number SNAS240B.

[20] F. Bizzarri, S. Callegari, and G. Gruosso, "Towards a nearly optimal synthesis of power bridge commands in the driving of AC motors," in *Proceedings of ISCAS 2012*, Seoul, May 2012.

[21] S. Callegari and F. Bizzarri, "Should ΔΣ modulators used in ac motor drives be adapted to the mechanical load of the motor?" in *Proceedings of IEEE ICECS 2012*, Seville (ES), Dec. 2012.

[22] S. Boyd and L. Vandenberghe, *Convex Optimization*, 7th ed. Cambridge University Press, 2009.

[23] W. L. Lee, "A novel high order interpolative modulator topology for high resolution oversampling A/D converters," Master's thesis, Massachussets Institute of Technology, 1987.

[24] K. C. H. Chao, S. Nadeem, W. L. Lee, and C. G. Sodini, "A higher order topology for interpolative modulators for oversampling A/D converters," *IEEE Trans. Circuits Syst.*, vol. 37, no. 3, pp. 309–318, Mar. 1997.

[25] A. Rantzer, "On the Kalman-Yakubovich-Popov lemma," *Systems & Control Letters*, vol. 28, no. 1, pp. 7–10, Jun. 1996.
[26] T. Iwasaki and S. Hara, "Generalized KYP lemma: Unified frequency domain inequalities with design applications," *IEEE Trans. Autom. Control*, vol. 50, no. 1, pp. 41–59, Jan. 2005.
[27] M. Osqui, M. Roozbehani, and A. Megretski, "Semidefinite programming in analysis and optimization of performance of Sigma-Delta modulators for low frequencies," in *Proc. of the American Control Conference*, Jul. 2007, pp. 3582–3587.
[28] U. Gustavsson, T. Eriksson, and C. Fager, "Quantization noise minimization in ΔΣ modulation based RF transmitter architectures," *IEEE Trans. Circuits Syst. I*, vol. 57, no. 12, pp. 3082–3091, Dec. 2010.
[29] R. M. Gray, "Toeplitz and circulant matrices: A review," *Foundations and Trends in Communications and Information Theory*, vol. 2, no. 3, pp. 155–239, 2006. [Online]. Available: http://ee.stanford.edu/~gray/toeplitz.pdf
[30] A. Antoniou, *Digital Filters: Analysis, Design and Applications*. McGraw-Hill, 2000.
[31] E. De Klerk, *Aspects of Semidefinite Programming: Interior Point Algorithms and Selected Applications*, ser. Applied Optimization. Kluwer, 2002.
[32] T. E. Oliphant, "Python for scientific computing," *IEEE Comput. Sci. Eng.*, vol. 9, no. 3, pp. 10–20, May 2007.
[33] M. Andersen, J. Dahl, Z. Liu, and L. Vandenberghe, "Interior-point methods for large-scale cone programming," in *Optimization for Machine Learning*, ser. Neural Information Processing series, S. Sra, S. Nowozin, and S. J. Wright, Eds. MIT Press, Sep. 2011, ch. 3, pp. 55–84. [Online]. Available: http://www.ee.ucla.edu/~vandenbe/publications/mlbook.pdf
[34] T. T. De Rubira, *CVXPY Documentation*, May 2012. [Online]. Available: http://www.stanford.edu/~ttinoco/cvxpy/
[35] M. Grant, S. Boyd, and Y. Ye, "Disciplined convex programming," in *Global Optimization: From Theory to Implementation*, ser. Nonconvex Optimization and its Applications, L. Liberti and N. Maculan, Eds. Springer, 2006, vol. 84, pp. 155–210. [Online]. Available: http://www.stanford.edu/~boyd/papers/pdf/disc_cvx_prog.pdf
[36] S. Boyd, L. El Ghaoui, E. Feron, and V. Balakrishnan, *Linear Matrix Inequalities in System and Control Theory*, ser. SIAM studies in applied mathematics. Philadelphia: SIAM, 1994, vol. 15.
[37] F. Zhang, Ed., *The Schur Complement and Its Applications*, ser. Numerical Methods and Algorithms. Springer, 2005, vol. 4.

Sergio Callegari (M'00–SM'06) received a Dr. Eng. degree (with honors) in electronic engineering and a Ph.D. degree in electronic engineering and computer science from the University of Bologna, Italy, in 1996 and 2000, respectively, working on the study of nonlinear circuits and chaotic systems. In 1996, he was a visiting student at King's College London, UK. He is currently a researcher and assistant professor at the School of Engineering II, University of Bologna, where he teaches Analog Electronics, Applied Analog Electronics and Sensing to students of Electronic Engineering and Aerospace Engineering. He is also a faculty member of the Advanced Research Center on Electronic Systems (ARCES) at the University of Bologna. In 2008, 2009, 2011 he was a visiting researcher at the University of Washington in Seattle for short periods. His current research interests include nonlinear signal processing, internally nonlinear, externally linear networks, chaotic maps, delta-sigma modulation, testing of analog circuits, and random number generation. Sergio Callegari has authored or co-authored more than 70 papers in international conferences, journals and scientific books, as well as 4 national patents. In 2004 he was co-recipient of the IEEE Circuit and Systems Society Darlington Award, for the best paper appeared in the IEEE Transactions on Circuits and Systems in the previous biennium. He served as an Associate Editor for the IEEE Transactions on Circuits and Systems — Part II during 2006–2007 and as an Associate Editor for the IEEE Transactions on Circuits and Systems — Part I during 2008–2009. He is a member of the Technical Committee on Nonlinear Circuits and Systems and of the Technical Committee on Education and Outreach of the IEEE CAS Society. He also served in the Organization Committee and as Publication Co-Chair at NOLTA 2006 (Bologna), as a member of the Organization Committee of Eurodoc 2006 (Bologna), as a Special-Session Co-Chair of NOLTA 2010 (Krakow) and as a Chair for the nonlinear circuits track at ICECS 2012. In 2005–2007, he has been a member of the board of the Italian Society of Doctoral Candidates and Ph.D. Graduates (ADI) and currently he is in the board of AIR, a national society for the promotion of scientific research.

Federico Bizzarri (M12) was born in Genoa, Italy, in 1974. He received the Laurea (M.Sc.) five-year degree (summa cum laude) in electronic engineering and the Ph.D. degree in electrical engineering from the University of Genoa, Genoa, Italy, in 1998 and 2001, respectively. Since June 2010 he has been a temporary research contract Assistant rofessor at the Electronic and Information Department of the Politecnico di Milano, Milan, Italy. In 2000 he was a visitor to EPFL, Lausanne, Switzerland. From 2002 to 2008 he had been a post-doctoral research assistant in the Biophysical and Electronic Engineering Department of the University of Genova, Italy. In 2009 he was a post-doctoral research assistant in the ARCES Research Center of the University of Bologna, Italy. His main research interests are in the area of nonlinear circuits, with emphasis on chaotic dynamics and bifurcation theory, circuit models of nonlinear systems, image processing, circuit theory and simulation. He is the author or coauthor of about 50 scientific papers, more than an half of which have been published in international journals.